Nuclear Engineering and Technology 53 (2021) 3229–3235

Contents lists available at ScienceDirect

Nuclear Engineering and Technology

journal homepage: www.elsevier.com/locate/net

Original Article

Experimental investigations and development of mathematical model to estimate drop diameter and jet length

Amitava Roy [a], G. Suneel [b, *], J.K. Gayen [b], K.V. Ravi [c], R.B. Grover [a]

[a] Homi Bhabha National Institute, Anushaktinagar, Mumbai, 400094, India
[b] Bhabha Atomic Research Center Facilities, Kalpakkam, Tamil Nadu, 603102, India
[c] Nuclear Recycle Board, Bhabha Atomic Research Centre, Mumbai, Maharashtra, 400085, India

ARTICLE INFO

Article history:
Received 23 November 2020
Received in revised form
13 April 2021
Accepted 9 May 2021
Available online 15 May 2021

Keywords:
Solvent extraction
Drop diameter
Jetting velocity
Jet length
Force balance
Mathematical model
Correlation comparison

ABSTRACT

The key process used in nuclear industries for the management of radiotoxicity associated with spent fuel in a closed fuel cycle is solvent extraction. An understanding of hydrodynamics and mass transfer is of primary importance for the design of mass transfer equipment used in solvent extraction processes. Understanding the interfacial phenomenon and the associated hydrodynamics of the liquid drops is essential for model-based design of mass transfer devices. In this work, the phenomenon of drop formation at the tip of a nozzle submerged in quiescent immiscible liquid phase is revisited. Previously reported force balance based models and empirical correlations are analyzed. Experiments are carried out to capture the process of drop formation using high-speed imaging technique. The images are digitally processed to measure the average drop diameter. A correlation based on the force balance model is proposed to estimate drop diameter and jet length. The average drop diameter obtained from the proposed model is in good agreement with experimental data with an average error of 6.3%. The developed model is applicable in both the necking as well as jetting regime and is validated for liquid-liquid systems having low, moderate and high interfacial tension.

1. Introduction

Solvent extraction is one of the most widely used separation processes in nuclear industry [1]. Liquid-liquid extraction is based on the partial miscibility of liquids. It is widely used in refining uranium and extraction of unused fissile, fertile material and other useful elements from the spent fuel. Reprocessing of the spent fuel not only reduces the radiotoxicity associated with the spent fuel but also provides radioisotopes for societal applications.

The transfer of mass from one liquid phase to the other depends on the interfacial area created by the dispersion of one liquid into another immiscible liquid. Understanding this phenomenon of dispersion is of prime importance in the design of liquid-liquid extraction systems. However, even today the design of industrial-scale extraction equipment relies on the studies carried out on pilot-scale equipment. The pilot-scale experiments usually consume most of the cost and time [2]. The need to achieve higher mass transfer efficiency in a compact extractor has become inevitable given the requirements of larger capacity process plants.

Pulsed perforated plate extraction column, one of the mass transfer equipment commonly used in nuclear reprocessing plants, has the advantage of higher level of controlled agitation for the creation of droplets, the dispersed phase. As a result, a large interfacial area is achieved resulting in higher mass transfer efficiency. To be successful in scale-up, robust and accurate models are required. The challenge in nuclear chemical engineering is to model the process in terms of mass and momentum transfer, the activity of the liquid, and anticipating the manifold and complex interactions in multiphase systems. In this regard, it is particularly useful to reduce the complexity of the swarm systems to single droplets since droplets are the smallest mass transfer unit in a liquid-liquid extraction device [3].

There have been developments in designing newer type of contactors with efficient mass transfer and phase separation. However, even today, industrial-scale plant design is based on the pilot plant experimental data and scale-up, sometimes with increased design margins. The model predicted design is yet to be proven for engineering scale adaptation before its final

* Corresponding author.
E-mail addresses: amitava05roy@yahoo.co.in (A. Roy), gattusuneelnrb@gmail.com (G. Suneel).

https://doi.org/10.1016/j.net.2021.05.008

acceptability for designing commercial equipment. Consequently, it has become necessary to gain an understanding of the hydrodynamics of a single drop and the associated physics so that the various design parameters could be established with better accuracy.

The phenomenon of drop formation in an immiscible, two-phase liquid–liquid system is primarily based on the balance between the competing lifting and restraining forces. The formation of liquid drops and their subsequent rise are important as they contribute significantly to the hydrodynamics in liquid-liquid contactors. The drop formation process controls drop size in the system and the drop rise velocity decides the characteristic contact time between the phases.

Many researchers attempted to understand the physics of drop formation employing force balance, numerical simulations and experimentation. Harkins and Brown [4] calculated the drop volume at very low flow rates by equating the buoyancy and interfacial tension forces. A correction for the fraction of liquid volume, which remains attached to the nozzle after drop break-off, was incorporated. The Harkins- Brown correction factor, which is empirical in nature, was used to obtain the drop volume at the time of break-off.

Hayworth et al. [5] as well as Null and Johnson [6] in their study, extended the work of Harkins and Brown, where velocity effect became an important parameter. Drag and inertial forces, which were incorporated into the force balance equations, predicted a semi-empirical correlation.

Klee and Treybal [7] carried out experiments on the rate of rise and fall of liquid drops by varying the densities of continuous and dispersed phases, interfacial tension, velocities, and thereby developed a correlation applicable for a wide range of systems. Narasinga Rao et al. [8] considered a two-stage drop formation mechanism in their model. In the two-stage drop formation mechanism, the drop formation process is divided into two stages; drop growth as the first stage and drop detachment as the second stage.

Scheele et al. [9] carried out a force balance and proposed model based on the two-stage drop formation mechanism and compared it with experimental investigations. Clift et al. [10] carried out the comprehensive review of drop formation and consolidated the experimental as well as the theoretical finding of drop formation. Mori et al. [11] carried out work on the pendant drop formation. Izard et al. [12] predicted drop diameter based on the force balances made across drop diameter. Chazal et al. [13] predicted drop diameter based on momentum balance. Suneel et al. [14] discussed the effect of bubbling with an immiscible medium on the throughput of vitrification equipment.

Although several sets of drop volume data exist in the literature [5,7,13,15–17] additional experiments are necessary to obtain a better understanding of the mechanism of drop formation and for validation of the model proposed in the present study. The study extends the range of variables studied earlier.

This work aims to investigate the drop formation mechanism that is, the initiation of drop formation, its growth, necking, and detachment at a lower velocity, and jet formation, jet instability, and jet break up into droplets at higher velocities. The prediction of drop detachment height or jet length, drop formation time, and drop diameter is also part of this investigation. In addition to experimental studies, numerical investigations are performed for single spherical drops under steady-state motion and in the laminar flow region. The study is confined to the formation of liquid drops from a submerged nozzle into an immiscible quiescent liquid.

The variation of the jet length with inlet velocity for various systems and the effect of jet length on drop diameter is not adequately addressed in the literature. The results are compared with the empirical correlations developed by Scheele et al. [9], Steiner et al. [18], Hamad et al. [15], Kagan et al. [19], Izard [12] and Chazal et al. [13] as these are intriguing in understanding the physics behind the drop formation. A review of the reported models for drop diameter based on force balance and analysis of findings of our experiments and simulations has resulted in proposing a new model, in which attempts are made to suitably address the observations made during the above study.

2. Materials and properties

Heptane, toluene, butyl acetate, 30% TBP in *n*-dodecane, and butanol were used as dispersed phase while deionized water was used as the continuous phase. The choice of dispersed phases was made to include a reasonable range of properties covering many scientific and engineering applications of the problem. The viscosities of the dispersed phases studied were in the range of 0.393 mPa.s to 2.52 mPa.s, while their densities and interfacial tensions were between 683 kg/m^3 to 882.5 kg/m^3 and 1.79 mN/m to 37.1 mN/m respectively. The properties of systems used in the current study at the temperature of 25 °C are given in Table 1.

3. Experimental setup and procedure

The schematic of the experimental set-up used for studying the mechanism of drop formation is shown in Fig. 1. The droplets are formed at the outlet of a submerged nozzle of 4 mm diameter. The test section consists of a cylindrical tank filled with continuous phase (c), into which a dispersed phase (di) is introduced through a nozzle attached to the bottom of the tank. To achieve precise control of the dispersed phase flow rate, it is fed from an organic feed tank pressurized by a controlled flow of air using a pre-calibrated control valve. The control valve is air operated and has linear characteristics. The valve is an air-to-open type and has a range of 1:20.

The free surface of the stationary continuous phase is 280 mm above the bottom of the test section. The nozzle used is machined out of stainless steel. A large length-diameter ratio is chosen to minimize disturbances and to assure a fully developed velocity profile at the nozzle exit. The nozzle penetrates 40 mm from the bottom of the test section into the continuous phase giving a distance of 240 mm from the nozzle exit to the free surface of the continuous phase The nozzle tip is machined flat so that undesirable wetting of the nozzle by the dispersed phase can be eliminated.

Drop diameters are measured from still photographs taken from a high-speed imaging system having a maximum shutter speed of 1000 frames/sec and resolution of 1280 × 1024 pixels. Two 500 W bulbs are used for illumination. Still images are taken for each drop emanating from the nozzle and the photographs are analyzed with digital imaging software. The images captured for Water (c) - *n*-Dodecane (di) are as shown in Fig. 2.

The diameter of the drop is determined by processing the captured images. For the cases in which the drop is deformed from a spherical shape, the drop diameter is recorded as the arithmetic average of the major and minor diameters. This procedure results in

Table 1
Properties of systems used for the study (T = 25 °C).

Dispersed phase	ρ_d (kg/m^3)	μ_d (mPa.s)	σ (mN/m)
Heptane	683	0.393	36.2
Toluene	870	0.59	37.1
Butyl acetate	882.5	0.685	12
30% TBP	842	1.92	9.5
Butyl alcohol	836	2.52	1.79

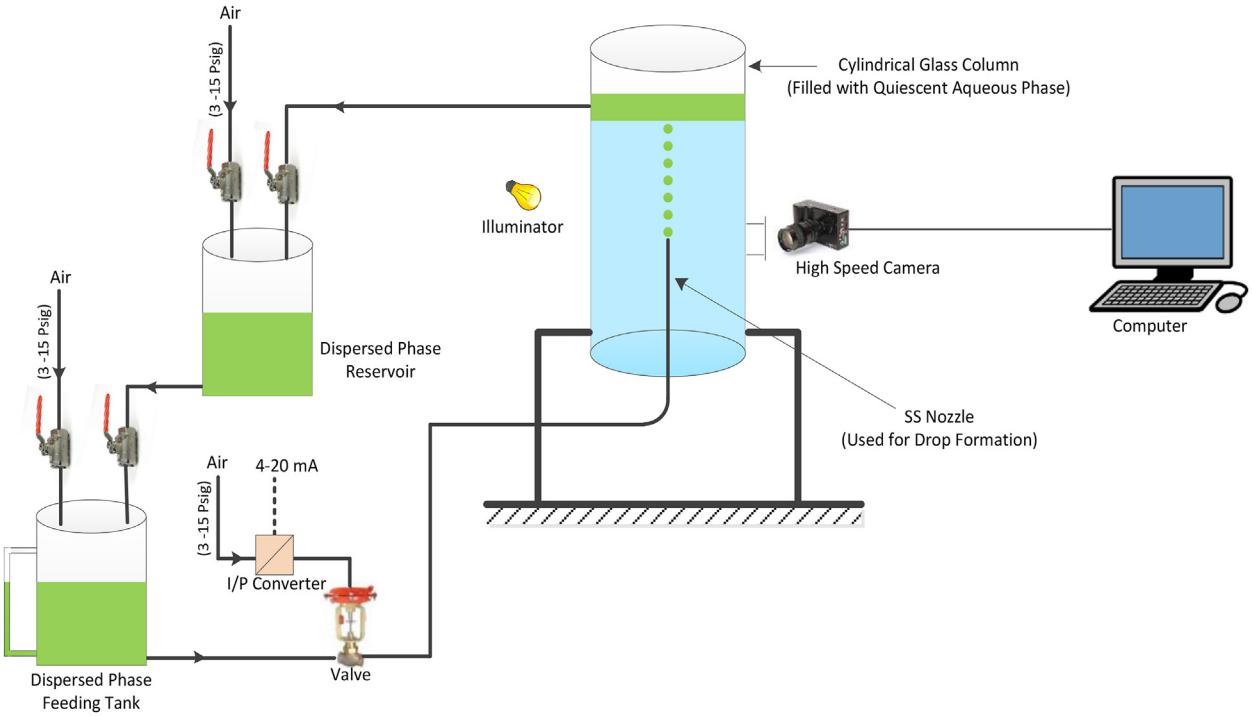

Fig. 1. The schematic diagram of the experimental set-up used for studying the mechanism of drop formation.

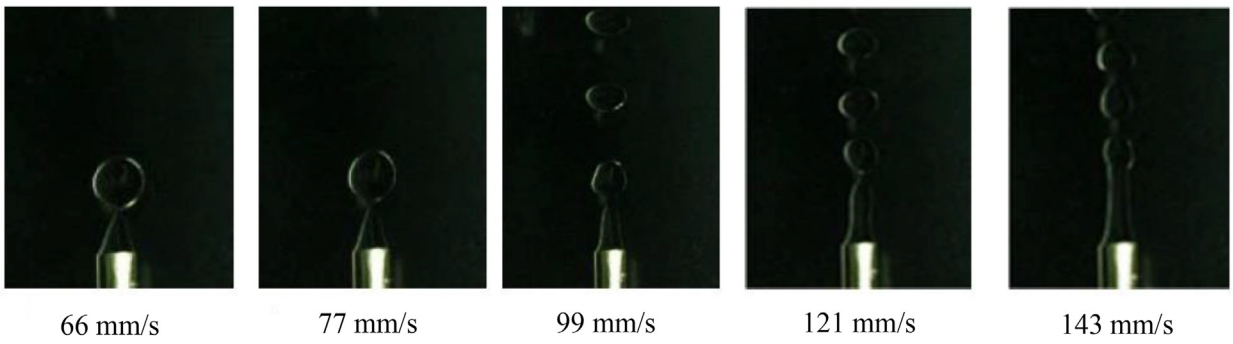

Fig. 2. Image captured with high frames speed camera at different inlet velocities for Water (c) - *n*-Dodecane (di) system.

less than 5% error in the calculation of drop volume provided the ratio of major-minor diameters is within 1.7. In this work, the ratio is less than 1.2 for most of the drops. The column is initially filled with de-ionized water and at instant t = 0, a dispersed phase is injected into the column through the nozzle. The superficial velocity of the disperse phase is varied within the range of 1.1–18.7 cm/s. The rise of ten bubbles is recorded using the video recorder.

4. Development of empirical correlation

The formation, growth, jetting, and detachment of a drop are due to the competing forces viz., the lifting and restraining forces acting on the drop. A simple model for drop formation in quiescent liquid under constant flow condition is proposed for calculating drop diameter and jet length for moderate flow rates of the dispersed phase.

The force balance of a single liquid drop emanating from a nozzle is shown in Fig. 3.

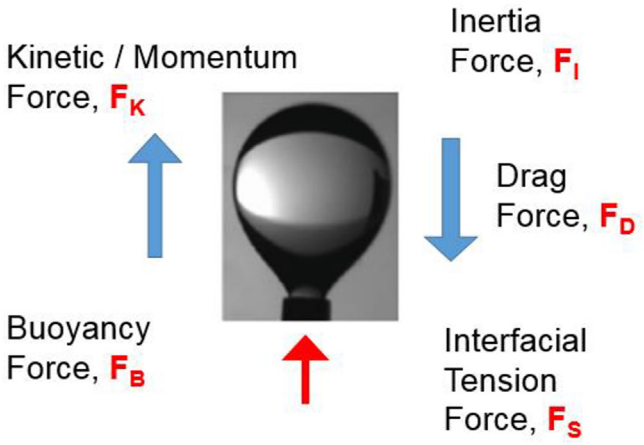

Fig. 3. The force balance of a single liquid drop emanating from a nozzle.

$$F_B + F_K = F_S + F_D + F_I \quad (1)$$

The following assumptions are made

a. The drop formation is a two-stage process.
b. No wall effect on the drop formation process.
c. The motion of the drop is not affected by the presence of another drop immediately above it.
d. The dispersed phase injection rate through the nozzle is constant and is incompressible.
e. The interface is acted upon by density difference between liquids and surface forces.
f. Drop detachment occurs when the neck narrows to zero.
g. The volumetric flow of dispersed phase is constant
h. The interfacial tension is constant and uniform.
i. There is no energy exchange or mass transfer across the interface.
j. Drop is axisymmetric.

The initiation of drop formation, its growth remaining attached to the nozzle, drop rise with neck, and subsequent detachment can be represented by two-stage force balance.

4.1. Growth Stage-1: Forces when the drop is attached to the nozzle

$$\text{Buoyancy Force,}\quad F_B = \Delta\rho V_1 g = \frac{4}{3}\pi r_1^3 \Delta\rho g \quad (2)$$

where $\Delta\rho$ is difference between dispersed and continuous phase densities, $|\rho_c - \rho_d|$ (kg/m^3), V_1 is drop volume at the end of stage-1 (m^3), g is the acceleration due to gravity (9.81), m/s^2 and r_1 is the radius of the drop in stage-1 (m).

$$\text{Kinetic Force,}\quad F_K = \rho_d dV\frac{dU_d}{dt} = \rho_d dV\frac{d}{dt}\left(\frac{Q}{\pi {R_N}^2}\right) = \rho_d Q dt\frac{d}{dt}\left(\frac{Q}{\pi {R_N}^2}\right) = \frac{Q^2\rho_d}{\pi {R_N}^2} \quad (3)$$

where, ρ_d is the density of dispersed phase (kg/m^3), V is drop volume at an instantaneous time, t (m^3), U_d is the velocity of the dispersed phase (m/s), Q is flow rate of the dispersed phase from the nozzle (m^3/s), and R_N is the radius of the nozzle (m).

$$\text{Interfacial tension Force,}\quad F_S = 2\pi\sigma R_N \cos\theta \quad (4)$$

where σ is interfacial tension coefficient (N/m).

F_S is the effective component of the interfacial tension force at the nozzle. As the drop grows, θ decreases and is zero at the time of drop detachment.

$$\text{Drag Force,}\quad F_D = \frac{1}{2}C_D A\rho_C {U_N}^2 \quad (5)$$

where, C_D is the drag coefficient, A is cross section area of the drop (m^2), ρ_C is the density of continuous phase (kg/m^3), and U_N is the velocity in the nozzle (m/s).

Drag Coefficient [20].

$$C_D(Re,\mu^*) = \frac{2-\mu^*}{2}C_D(Re,0) + \frac{4\mu^*}{6+\mu^*}C_D(Re,2) \quad 5 \le Re \le 1000;$$

$$0 \le \mu^* \le 2 \quad (6)$$

where, Re is Reynolds Number, and μ^* is the ratio of viscosities of dispersed and continuous phase - μ_d/μ_c, μ_c is the viscosity of continuous phase (Pa.s), and μ_d is the viscosity of dispersed phase (Pa.s).

$$C_D(Re,0) = \frac{48}{Re}\left(1 + \frac{2.21}{\sqrt{Re}} - \frac{2.14}{Re}\right)$$

$$C_D(Re,2) = 17Re^{-2/3}$$

$$Re = dU_N\rho_c/\mu_c$$

$$\text{Inertia Force,}\quad F_I = \frac{d}{dt}(mV_1U_N) = m\frac{d}{dt}\left(\frac{4}{3}\pi r_1^3\right) \times \left(\frac{Q}{4\pi r_1^2}\right) = \frac{1}{3}mQ\frac{dr_1}{dt} = \frac{mQ^2}{12\pi r_1^2} \quad (7)$$

where m is the virtual mass coefficient, $\rho_d + 0.5\rho_c$ (kg/m^3).

Thus, the final expression for force balance at the end of stage 1

$$\frac{4\pi}{3}\Delta\rho g r_1^3 + \frac{Q^2\rho_d}{\pi R_N^2} - 2\pi\sigma R_N - F_D = \frac{mQ^2}{12\pi r_1^2} \quad (8)$$

Equation (8) can be used to obtain the diameter of the drop at the end of stage-1, which is when the forces are in balance.

The drop starts moving upward at the end of stage-1 when the lifting forces are higher than the restraining forces, that is under the condition of

$$\frac{4\pi}{3}\Delta g r_1^3 + \frac{Q^2\rho_d}{\pi R_N^2} > 2\pi R_N\sigma - F_D + \frac{mQ^2}{12\pi r_1^2}$$

4.2. Stage-2: Forces at the time of detachment and during drop rise

In Stage-2, the drop is fully formed and it detaches when a sufficient amount of the additional liquid has flowed into the drop through its neck leading to force imbalance and drop detaches leaving some volume at the tail back on the nozzle. The forces at the time of detachment are

$$\Delta\rho V_2 g + \frac{Q^2\rho_d}{\pi r_2^2} - 2\pi\sigma r_2 - F_D = \frac{d}{dt}(mV_2U) \quad (9)$$

where, V_2 is drop volume at the end of stage-2 (m^3), and r_2 is the radius of the drop in stage-2 (m)

$$U = \frac{dx}{dt} + \frac{dr_2}{dt}$$

$$\frac{d}{dt}(mV_2U) = \frac{d}{dt}\left(mV_2\left(\frac{dx}{dt} + \frac{dr_2}{dt}\right)\right) = \frac{mQ^2}{12\pi r_2^2} + \frac{d}{dt}\left(mV_2\left(\frac{dx}{dt}\right)\right) \quad (10)$$

At the time of the drop detachment, a fraction of volume is retained back on the nozzle due to recoil force. This volume of the drop that remained at the nozzle after drop breakup was not considered by Hamad et al. [15]. By using a correction factor for the volume of the liquid drop, it can be incorporated into the equation. Hence, a correction factor ψ called 'Harkin–Browns Correction

factor' is introduced into the equation for finding the actual force on the detaching drop. This correction factor accounts for the volume of the drop left on the nozzle at the time of detachment.

Substituting Equation (9) into (10) and introducing ψ

$$\psi\left[\Delta\rho V_2 g+\frac{Q^2\rho_d}{\pi r_2^2}-2\pi\sigma r_2-F_D-\frac{mQ^2}{12\pi r_2^2}\right]=\frac{d}{dt}\left(mV_2\frac{dx}{dt}\right) \tag{11}$$

The jet length 'x' is obtained by integrating the right-hand side of Equation (11) from t = 0 to t = t.

The length of the liquid between the top of the detaching drop and nozzle tip is called the jet length. Jet length is predicted by Scheele et al. [21].

$$x=\frac{1}{2\alpha}\left[\left(\frac{a^2U_I}{R_N^2}\right)_{\bar{Z}=5}+\left(\frac{a^2U_I}{R_N^2}\right)_{Z=x}\right]\ln\left(\frac{R_N}{\varepsilon}\right) \tag{12}$$

where 'a' is the radius of the jet (m), U_I is the interfacial velocity of the jet (m/s), α is the growth rate of disturbance (s^{-1}), Z is the axial distance of jet (m), and ε is the thickness of the interphase (m).

The complex dependence of interfacial velocity (U_I) on the axial distance of the nozzle precludes an analytical solution for jet length. The interfacial velocity does not change rapidly with distance from the nozzle exit after a sharp initial increase, so an arithmetic average of interfacial velocities at $\bar{Z}=5$ and Z = x provides a satisfactory estimate of the interfacial velocity [21].

Substituting Equations (9)–(11) in Equation (8) and integrating the equation so obtained will lead to the following algebraic equation which can be used to determine the drop diameter at the end of stage-2 by incorporating the volume correction factor:

$$\begin{aligned}&\psi\left[\frac{A}{4Q^2}\left(V_2^2-V_1^2\right)+B_1\left\{\frac{(V_2-V_1)}{Q^2}-\frac{V_1}{Q^2}\ln\left(\frac{V_2}{V_1}\right)\right\}\right.\\&+C_1\left\{V_2^{4/3}-V_1^{4/3}\right\}+C_2\left\{V_2^{7/6}-V_1^{7/6}\right\}+C_3\left\{V_2^{13/9}-V_1^{13/9}\right\}\\&+C_4\{V_2-V_1\}-\frac{1}{Q}\left\{V_1^{4/3}\log\frac{V_2}{V_1}+V_1^{7/6}\log\frac{V_2}{V_1}+V_1^{13/9}\log\frac{V_2}{V_1}\right\}\\&\left.-\frac{9D}{Q^2}\left\{V_2^{1/3}-V_1^{1/3}\right\}-\frac{E}{Q}\ln\left(\frac{V_2}{V_1}\right)\right]=x\end{aligned} \tag{13}$$

where,

$$A=\frac{\Delta\rho g}{m},\quad B_1=\frac{\left(\frac{Q^2\rho_d}{\pi R_N^2}-2\pi\sigma\left(\left(\frac{3V_2}{4}\right)^{1/3}\right)\right.}{m},$$

$$C_1=\frac{\frac{\left(432\left\{12-\mu^{*2}-4\mu^*\right\}U_N\rho_c/\mu_c\right)}{\left(\left\{\frac{U_N\rho_c}{\mu_c}\right\}^2\right)}\left(\frac{6}{\pi}\right)^{\frac{1}{3}}\pi U_N\frac{\rho_c}{2}}{16mQ^2},$$

$$C_2=\frac{\frac{\left(3818.88\left\{12-\mu^{*2}-4\mu^*\right\}\sqrt{\frac{U_N\rho_c}{\mu_c}}\right)}{\left(\left\{\frac{U_N\rho_c}{\mu_c}\right\}^2\right)}\left(\frac{6}{\pi}\right)^{\frac{1}{3}}\pi U_N\frac{\rho_c}{2}}{49mQ^2},$$

$$C_3=\frac{81.13\mu^*\left(\frac{U_N\rho_c}{\mu_c}\right)^{-\frac{2}{3}}\cdot\left(\frac{6}{\pi}\right)^{\frac{1}{3}}\cdot\pi U_N\frac{\rho_c}{2}}{169mQ^2},$$

$$C_4=\frac{\frac{\left(2.14\cdot48\left\{12-\mu^{*2}-4\mu^*\right\}\right)}{\left(\left\{\frac{U_N\rho_c}{\mu_c}\right\}^2\right)}\cdot\pi U_N\frac{\rho_c}{2}}{mQ^2},\quad D=\frac{Q^2}{12\pi(3/4\pi)^{2/3}}$$

$$\&\quad E=\frac{A}{2Q}V_1^2-\frac{2C}{Q}V_1^{\frac{1}{2}}-\frac{3D}{Q}V_1^{\frac{1}{3}}$$

The developed equation is solved iteratively using the Newton-Raphson method with a solution tolerance of 10^{-6}.

5. Results and discussion

5.1. Jet Length

As the injection velocity of the dispersed phase increases, the jet length increases for all the systems as shown in Fig. 4. In this study, jet length was predicted using available correlations for different systems viz., Water (c) - Butyl acetate (di), Water (c) - Toluene (di), Water (c) - 30% TBP (di) and Water (c) - Dodecane (di). It was observed that systems with lower interfacial tension form jet at lower velocities. The obtained jet lengths were incorporated in correlation, Equation (13), for the determination of drop diameter for respective systems.

5.2. Drop diameter

The studies were carried out with a 4 mm nozzle, using water as a continuous phase and different solutions as a dispersed phase. The inlet velocity of the dispersed was varied from 11 mm/s to 70 mm/s. Experimental data of Scheele et al. [9], is used for the Heptane system. Experimental results are compared with simulations and correlations developed by Scheele et al. [9], Hamad et al. [15], Steiner et al. [18], Kagan et al. [19], Chazal et al. [13], Izard [12] and a correlation is proposed using developed force balance as shown in Fig. 5 for various liquid-liquid systems.

As can be seen in Fig. 5, the agreement of the model with experiments is better at lower velocities. The agreement of the model is ±6.2% up to a velocity of 40 mm/s. The disagreement of the model with experimental data at higher velocities may be due to jet instabilities that occur at higher velocities. The present model has a better agreement compared with the empirical correlations.

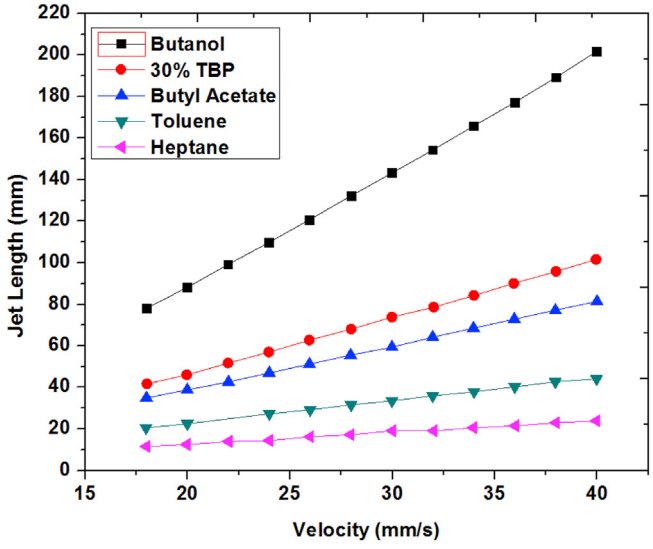

Fig. 4. Effect of Interfacial Tension on Jet length for different systems.

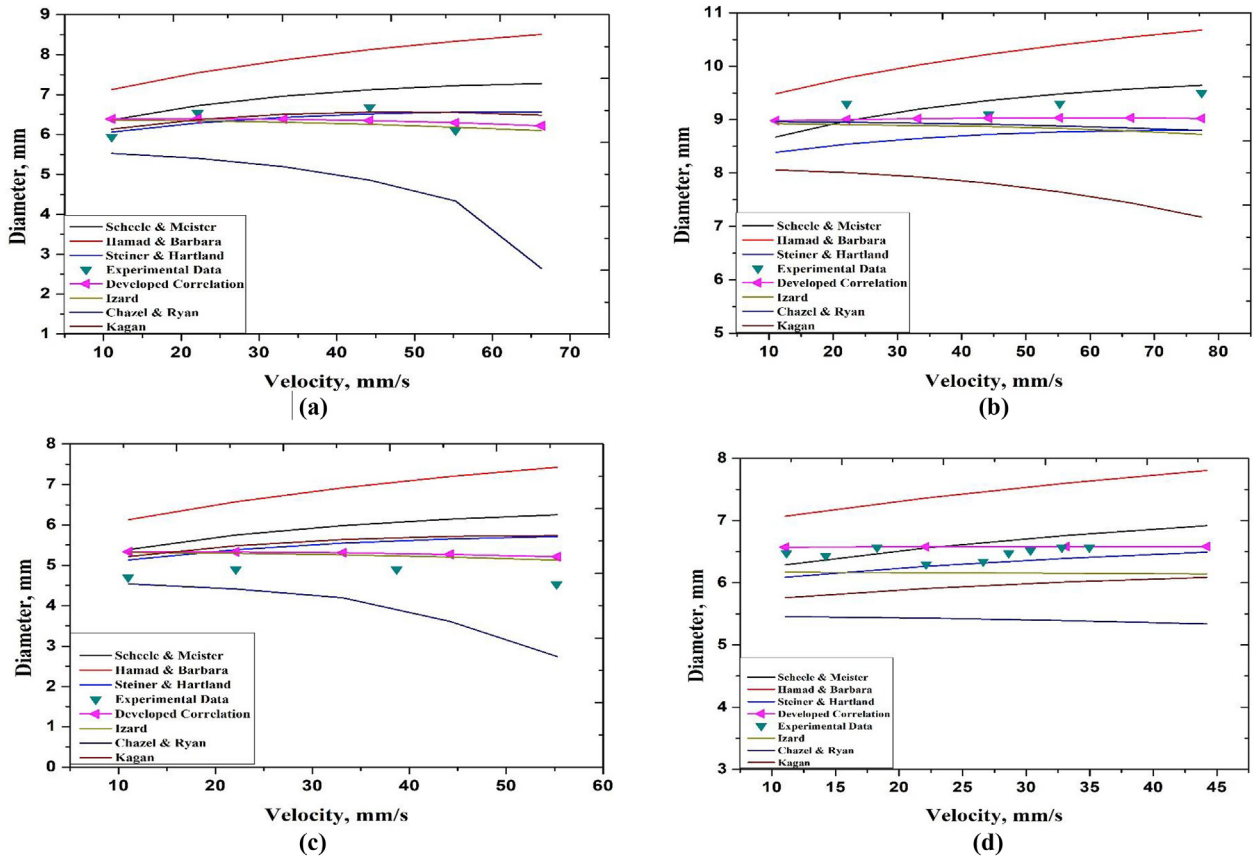

Fig. 5. Comparison of drop diameters obtained from experiment, and mathematical model for (a) Water (c) - Butyl acetate (di), (b) Water (c) - Toluene (di) (c) Water (c) - 30% TBP (di), (d) Water (c) - Heptane (di) system.

5.3. Error analysis

To give a quantitative idea of the performance of Equation (13) data-driven correlation, a statistical term, coefficient of determination (COD) was introduced. The value of COD for the data was found to be 0.98 for Water – Butyl acetate/Toluene/Heptane/30% TBP-dodecane for proposed correlation. This estimated drop diameters from the developed correlation for the given systems have a better agreement compared to the correlations reported in the literature. The parity plot of predicted drop diameters for various systems is shown in Fig. 6.

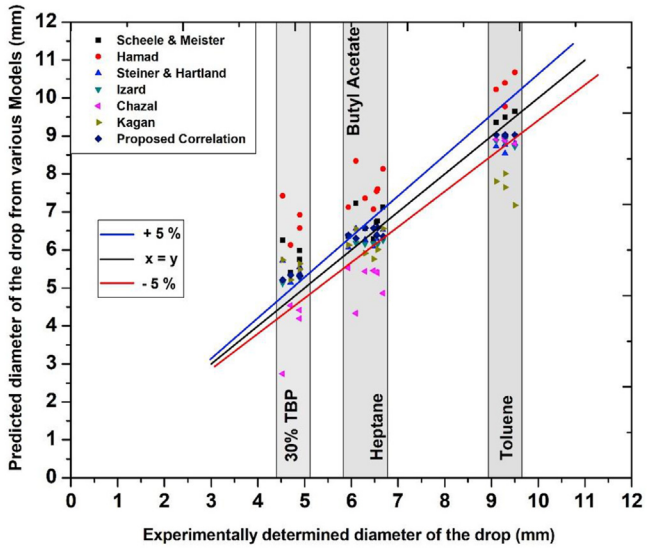

Fig. 6. Parity plot for Water – Toluene/Butyl acetate/30% TBP-dodecane/Heptane system.

6. Conclusions

Models based on force balance on a single drop of the dispersed phase emanating from a nozzle submerged in a quiescent immiscible ambient liquid phase were studied. Experiments were carried out to study the different stages of drop formations viz., initiation of drop formation at the tip of the nozzle, its growth, necking, jetting and drop detachment, which were captured by high-speed videography. A new model for drop diameter and jet length is proposed for the two-stage drop formation mechanism by introducing drop volume correction (using ψ) and interfacial terms, drag coefficient (C_D) and the analytical expression for jet length (x). Jet length and drop diameter were determined by processing the captured images. The two-phase systems studied are (i) Toluene, (ii) 30% TBP in dodecane, (iii) Dodecane and (iv) Butyl acetate as the dispersed phase and water as the quiescent continuous phase. Drop diameters predicted by the developed correlation for different systems, at varying dispersed phase velocity through the nozzle are in good agreement with experimental results, with an average error of ±5%. Drop diameters obtained from the proposed model are in good agreement with the experimental data having COD of 0.98. The model is applicable in the jetting regime and is validated for two-phase systems with low, moderate and high interfacial

tension. Considering the applicability of the proposed model for a wide range of systems properties, higher velocities, a lesser degree of empiricism and system independence, it will be useful for enhancing the drop level understanding of hydrodynamic and mass transfer phenomenon in liquid-liquid extraction equipment.

Declaration of competing interest

The authors declare that they have no known competing financial interests or personal relationships that could have appeared to influence the work reported in this paper.

Appendix A. Supplementary data

Supplementary data related to this article can be found at https://doi.org/10.1016/j.net.2021.05.008.

References

[1] A. Roy, M. Darekar, K.K. Singh, K.T. Shenoy, R.B. Grover, Drop formation at nozzles submerged in quiescent continuous phase: an experimental study with TBP-dodecane and nitric acid system, Nucl. Sci. Tech. 29 (6) (2018), https://doi.org/10.1007/s41365-018-0415-z.
[2] J. Zhang, Y. Wang, G.W. Stevens, W. Fei, A state-of-the-art review on single drop study in liquid-liquid extraction: experiments and simulations, Chin. J. Chem. Eng. 27 (12) (2019) 2857–2875, https://doi.org/10.1016/j.cjche.2019.03.025.
[3] M. Wegener, N. Paul, M. Kraume, Fluid dynamics and mass transfer at single droplets in liquid/liquid systems, Int. J. Heat Mass Transf. 71 (2014) 475–495.
[4] W.D. Harkins, F.E. Brown, The determination of surface tension (free surface energy), and the weight of falling drops: the surface tension of water and benzene by the capillary height method, J. Am. Chem. Soc. 41 (4) (1919) 499–524, https://doi.org/10.1021/ja01461a003.
[5] C.B. Hayworth, R.E. Treybal, Drop formation in two-liquid-phase systems, Ind. Eng. Chem. 42 (6) (1950) 1174–1181, https://doi.org/10.1021/ie50486a030.
[6] H.R. Null, H.F. Johnson, Drop formation in liquid-liquid systems from single nozzles, AIChE J. 4 (3) (1958) 273–281, https://doi.org/10.1002/aic.690040308.
[7] A.J. Klee, R.E. Treybal, Rate of rise or fall of liquid drops, AIChE J. 2 (4) (1956) 444–447, https://doi.org/10.1002/aic.690020405.
[8] E.V.L. Narasinga Rao, R. Kumar, N.R. Kuloor, Drop formation studies in liquid-liquid systems, Chem. Eng. Sci. 21 (10) (1966) 867–880, https://doi.org/10.1016/0009-2509(66)85081-9.
[9] G.F. Scheele, B.J. Meister, Drop formation at low velocities in liquid-liquid systems: Part I. Prediction of Drop Volume, AIChE J. 14 (1) (1968) 9–15.
[10] R. Clift, J.R. Grace, M.E. Weber, M.F. Weber, Bubbles, Drops, and Particles, Academic Press, 1978.
[11] Y.H. Mori, Harkins-Brown correction factor for drop formation, AIChE J. 36 (8) (1990) 1272–1274.
[12] J.A. Izard, Prediction of drop volumes in liquid-liquid systems, AIChE J. 18 (3) (1972) 634–638.
[13] L.E.M. de Chazal, J.T. Ryan, Formation of organic drops in water, AIChE J. 17 (5) (1971) 1226–1229, https://doi.org/10.1002/aic.690170531.
[14] G. Suneel, C.P. Kaushik, P.M. Satya Sai, J.K. Gayen, K.V. Ravi, Enhancement of glass production rate in Joule heated ceramic melter, Chem. Prod. Process Model (2019) 1–11, https://doi.org/10.1515/cppm-2019-0068.
[15] F.A. Hamad, M.K. Khan, B.K. Pierscionek, H.H. Bruun, Comparison of experimental results and numerical predictions of drop diameter from a single submerged nozzle in a liquid-liquid system, Can. J. Chem. Eng. 79 (3) (2001) 322–328, https://doi.org/10.1002/cjce.5450790304.
[16] R.E. Treybal, F.E. Dumoulin, Liquid-liquid extraction in a perforated plate tower - effect of plate spacing on tower performance, Ind. Eng. Chem. 34 (6) (1942) 709–713, https://doi.org/10.1016/0015-1882(91)80255-4.
[17] C.T. Chen, J.R. Maa, Y.M. Yang, C.H. Chang, Drop formation from flat tip nozzles in liquid-liquid system, Int. Commun. Heat Mass Tran. 28 (5) (2001) 681–692, https://doi.org/10.1016/S0735-1933(01)00272-X.
[18] L. Steiner, S. Hartland, Handbook of Fluids in Motion, Ann Arbor Science, Michigan, 1983.
[19] S.Z. Kagan, Y.N. Kovalev, A.P. Zakharychev, Drop size in spray nozzle eflux in liquid-liquid systems, TOKhT VII (4) (1974) 565–570.
[20] Z.G. Feng, E.E. Michaelides, Drag coefficients of viscous spheres at intermediate and high Reynolds numbers, J. Fluid. Eng. 123 (4) (2001) 841–849, https://doi.org/10.1115/1.1412458.
[21] B.J. Meister, G.F. Scheele, Prediction of jet length in immiscible liquid systems, AIChE 15 (5) (1969) 689–706.